JCB Article

Knockdown of the survival motor neuron (Smn) protein in zebrafish causes defects in motor axon outgrowth and pathfinding

Michelle L. McWhorter,[1,2] Umrao R. Monani,[3] Arthur H.M. Burghes,[2,3,4,5] and Christine E. Beattie[1,2,6]

[1]Center for Molecular Neurobiology, [2]Molecular, Cellular, and Developmental Biology Program, [3]Department of Neurology, [4]Department of Molecular and Cellular Biochemistry, [5]Department of Molecular Genetics, and [6]Department of Neuroscience, The Ohio State University, Columbus, OH 43210

Spinal muscular atrophy (SMA) is an autosomal recessive disorder characterized by a loss of α motoneurons in the spinal cord. SMA is caused by low levels of the ubiquitously expressed survival motor neuron (Smn) protein. As it is unclear how low levels of Smn specifically affect motoneurons, we have modeled SMA in zebrafish, a vertebrate model organism with well-characterized motoneuron development. Using antisense morpholinos to reduce Smn levels throughout the entire embryo, we found motor axon–specific pathfinding defects. Reduction of Smn in individual motoneurons revealed that *smn* is acting cell autonomously. These results show for the first time, in vivo, that Smn functions in motor axon development and suggest that these early developmental defects may lead to subsequent motoneuron loss.

Introduction

Zebrafish is an excellent organism for studying human disease (Dodd et al., 2000) due to its well-characterized embryonic development and the ability to perform both forward and reverse genetics (for review see Grunwald and Eisen, 2002). Protein knockdown technology has facilitated analysis of zebrafish forms of muscular dystrophy (Parsons et al., 2002) and cystic kidney disease (Liu et al., 2002). Due to its well-characterized nervous system and relatively simple neuromuscular organization, zebrafish are well suited for analysis of neuromuscular diseases. Taking advantage of these attributes, we have used protein knockdown in zebrafish to model spinal muscular atrophy (SMA).

SMA, an autosomal recessive disorder, is the leading hereditary cause of infant mortality (Roberts et al., 1970) and is characterized by loss of α motoneurons in the spinal cord (Crawford and Pardo, 1996; Melki, 1997). The disease results from low levels of the protein encoded by the survival motor neuron (*SMN*) gene. Although SMN is expressed in all cell types, motoneurons are specifically affected in SMA, indicating their sensitivity to low SMN levels (Coovert et al., 1997; Lefebvre et al., 1997; Monani et al., 2000). Humans have two copies of the *SMN* gene, *SMN1* and *SMN2*, which differ in a single base change in a splice enhancer site for exon 7 of *SMN2* (Lorson et al., 1999; Monani et al., 1999; Cartegni and Krainer, 2002). Thus, *SMN1* produces a majority of full-length transcript, whereas *SMN2* generates mostly transcripts lacking exon 7, although some full-length transcript is produced (Lefebvre et al., 1995). SMN protein lacking exon 7 does not oligomerize effectively (Lorson and Androphy, 1998) and appears to be unstable and rapidly degraded (Lorson and Androphy, 2000). Thus, mutations in *SMN1,* but retention of the *SMN2* gene, results in reduced protein levels and ultimately SMA (Lefebvre et al., 1995, 1997; Coovert et al., 1997).

The 38-kD SMN protein is ubiquitously expressed and localizes to both the cytoplasm and nucleus (Liu and Dreyfuss, 1996; Coovert et al., 1997; Lefebvre et al., 1997). In the nucleus, SMN localizes to structures termed gems, which overlap or are in close proximity to coiled bodies (Liu and Dreyfuss, 1996; Young et al., 2000a). It has been termed the master RNA assembler and, in particular, has been shown to be important in assembly of snRNP particles (for review see Terns and Terns, 2001). SMN also binds to the hn-RNP-R,

The online version of this article includes supplemental material.

Address correspondence to Christine E. Beattie, Center for Molecular Neurobiology, The Ohio State University, 115 Rightmire Hall, 1060 Carmack Road, Columbus, OH 43210. Tel.: (614) 292-5113. Fax: (614) 292-5379. email: beattie.24@osu.edu

Key words: SMA; SMN; motoneurons; zebrafish; morpholino

Abbreviations used in this paper: AChR, acetylcholine receptor; CaP, caudal primary; MO, morpholino oligonucleotide; SMA, spinal muscular atrophy; SMN, survival motor neuron; VeLD, ventral longitudinal descending.

which is involved in RNA editing and mRNA transport (Rossoll et al., 2002). Recent data shows that hn-RNP-R colocalizes with SMN in distal axons of embryonic motoneurons (Jablonka et al., 2001; Rossoll et al., 2002). SMN also has been shown to localize in the growth cones and branch points of developing neurons (Jablonka et al., 2001; Fan and Simard, 2002; Zhang et al., 2003). Ultimately, however, the function of SMN in relation to SMA pathology and etiology remains unclear.

To further analyze SMN function, animal models of SMA have been generated (Schrank et al., 1997; Hsieh-Li et al., 2000; Monani et al., 2000; Cifuentes-Diaz et al., 2002; Monani et al., 2003). In contrast to humans, mice have only one *Smn* gene, which is equivalent to human *SMN1* (DiDonato et al., 1997; Viollet et al., 1997). Complete loss of this gene results in an embryonic lethal phenotype (Schrank et al., 1997). Introduction of one or two copies of human *SMN2* rescues the embryonic lethal phenotype and results in mice with severe SMA (Hsieh-Li et al., 2000; Monani et al., 2000), whereas 8–16 copies of *SMN2* completely rescue the SMA phenotype (Monani et al., 2000). Although both severe and mild SMA mice ultimately exhibit motoneuron cell body reduction (Monani et al., 2000, 2003), no early morphological or biochemical abnormality of the motoneurons has been reported.

A model of SMA in zebrafish has the potential to elucidate the effect of decreased Smn levels on motoneuron development in vivo. At 24 h, there are three well-characterized primary motoneurons per spinal cord hemisegment that innervate either the dorsal, rostral, or ventral region of each myotome (Eisen et al., 1986; for review see Beattie, 2000; Fig. S1, available at http://www.jcb.org/cgi/content/full/jcb.200303168/DC1). Over the next few days, each of the primary motor axons are joined by 20–30 secondary motor axons, which form three distinct nerves that innervate the three myotome regions (Myers et al., 1986; Pike et al., 1992). As these axons extend into defined myotome regions, they can be followed in living embryos; thus, perturbations in the organization of these neurons or their axons can be readily detected, followed during development, and quantitated (for review see Beattie, 2000).

We have used antisense morpholino technology to model the effects of low levels of *smn* in zebrafish. Reducing Smn protein levels in the developing embryo results in motor axon–specific truncations and branches, independent of motoneuron cell death. Moreover, by decreasing Smn levels in single motoneurons, we show that these defects are due to a cell-autonomous function of Smn in motoneurons. These are the first reported morphological abnormalities of motoneuron development in response to low levels of Smn. These data reveal that one of the earliest consequences of Smn protein reduction is severely compromised motor axon outgrowth, indicative of an essential role for Smn in motoneuron development.

Results

Mapping and expression of *smn*

The zebrafish *smn* gene was mapped to linkage group 5 on the LN 54 radiation hybrid panel (Hukriede et al., 1999). Southern blot and radiation hybrid mapping (unpublished data) indicated that there is only a single *smn* gene in zebrafish. RNA in situ hybridization showed that, like its mammalian counterpart, zebrafish *smn* appears to be expressed in all cell types based on diffuse and ubiquitous staining at 22, 27, 36, and 48 h after fertilization (h; Fig. S2, available at http://www.jcb.org/cgi/content/full/jcb.200303168/DC1).

Knockdown of Smn causes spinal motor axon defects

Morpholino antisense oligonucleotide "knockdown" technology was performed in zebrafish to decrease the levels of the Smn protein and mimic SMA. Morpholino oligonucleotides (MOs) inhibit the translation of their target mRNA, thereby causing reduced levels of target protein (Nasevicius and Ekker, 2000). Control or *smn* MO was injected into embryos at the one- to four-cell stage, and then embryos were allowed to develop until the desired time. Western blot analysis showed that *smn* MO–injected embryos exhibited a 61% decrease in Smn protein at 36 h (Fig. 1, A and B). Approximately 78% ($n = 580$) of embryos injected with 6 ng of *smn* MO survived compared with 91% ($n = 139$) survival when injected with the same concentration of control MO. Embryos died between late gastrulation and early somitogenesis, suggesting essential Smn function during zebrafish development. *smn* MO–injected embryos that survived did not exhibit gross abnormalities.

Initial examination focused on a subset of primary motoneurons. Cell bodies of caudal primary (CaP) and variable primary (VaP) motoneurons are located in the middle of each spinal cord hemisegment and express the LIM gene *islet2* (Appel et al., 1995). Using *islet2* RNA in situ hybridization, we found that these motoneurons were present in both control MO ($n = 6$) and *smn* MO–injected embryos ($n = 42$; unpublished data). Using the znp1 mAb, we examined CaP motor axons. At 27 h, CaP axon projections have a stereotyped morphology and project into ventral muscle, as shown in a control MO–injected embryo (Fig. 1 C). *smn* MO–injected embryos, however, showed motor axon defects that could be grouped into two categories based on axon length and axon branching. Approximately 35.3% of *smn* MO–injected embryo sides had at least one truncated motor axon that did not fully project into the ventral muscle (Table I; Fig. 1 D). Affected sides in *smn* MO–injected embryos had an average of 1.90 truncated axons (Table II). Axon branching was also observed in *smn* MO–injected embryos. At 27 h, 14.3% of embryo sides had at least one branched axon (Table I; Fig. 1 E), and each affected side had an average of 2.31 branches (Table II). These defects were typically found between hemisegments 5 and 17, corresponding to middle through posterior trunk. It was rare that axon defects were seen along the proximal portion of the axon, between the ventral root and the first intermediate target at the nascent horizontal myoseptum (Fig. 1, white arrowhead).

By 36 h, secondary motor axons also extend into the ventral muscle and fasciculate to form a nerve (Fig. 1 F). At 36 h in *smn* MO–injected embryos, 61.5% of the sides had at least one truncated axon (Table I; Fig. 1 G), compared with 35.3% at 27 h. Affected sides had an average of 2.81 trun-

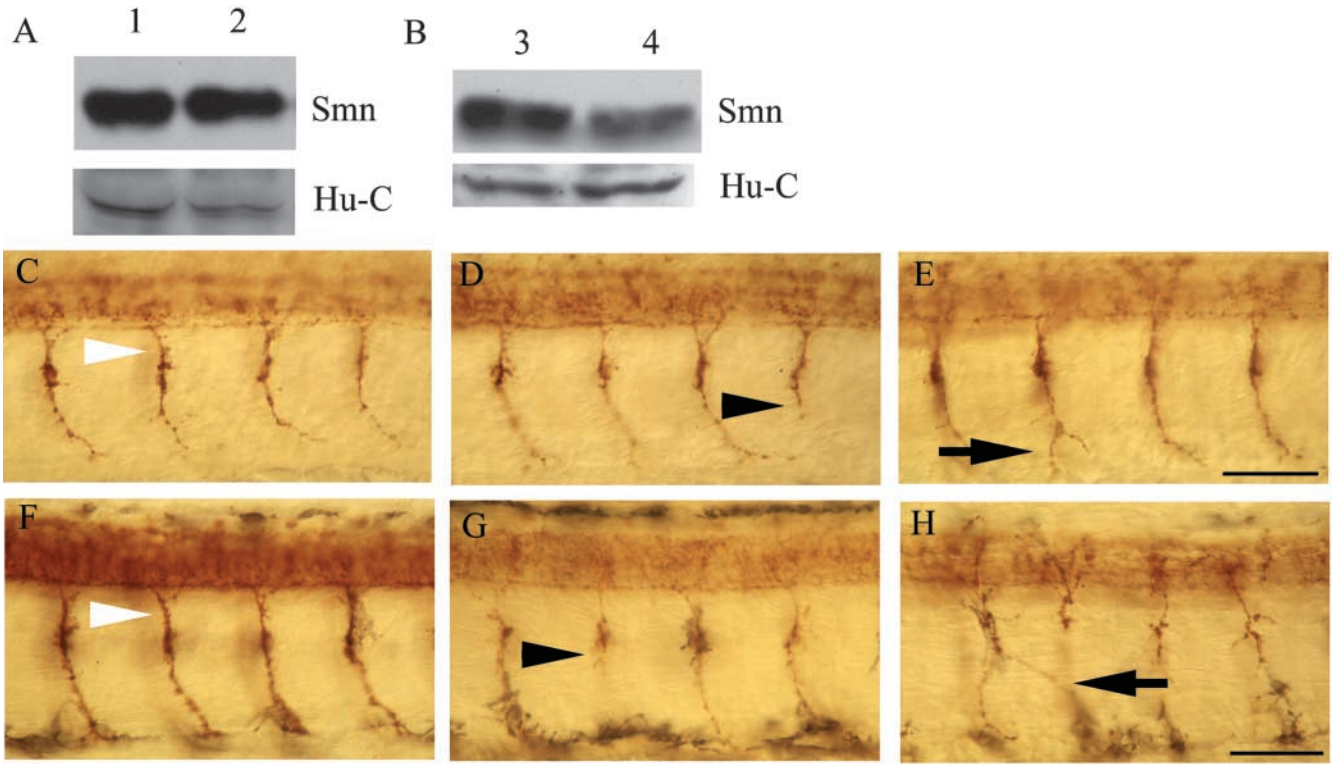

Figure 1. **Motor axons/nerves are abnormal in embryos injected with 6 ng of *smn* MO.** Western blot analysis of WT uninjected (lanes 1 and 3), control MO–injected (lane 2), and *smn* MO–injected (lane 4) embryos at 36 h (Smn is 37–38 kD). Hu-C, a neuronal marker, is shown as a loading control. Lateral views (anterior to the left; dorsal to the top) of whole-mount embryos labeled with znp1 mAb at 27 (C–E) and 36 h (F–H) in embryos injected with control MO (C and F) or *smn* MO (D, E, G, and H). Truncated motor axons/nerves (D and G; black arrowheads) and branched motor axons/nerves (E and H; black arrows) occur. White arrows demarcate the proximal axon pathway (C and F). Bars: (C–E) 25 μm; (F–H) 30 μm.

cated nerves, which is consistent with what was observed at 27 h (Table II). However, at 36 h, there were more sides with increased numbers of truncated nerves. 44.6% of the sides in *smn* MO–injected embryos had at least one branched nerve (Table I; Fig. 1 H) in contrast to only 23.6% at 27 h. The average number of branches per side remained constant at 2.5 (Table II).

Further knockdown of Smn protein results in increased motor axon branching

It has been shown in human patients and mouse models that the severity of SMA is dependent on the amount of SMN protein (Monani et al., 2000). To investigate if motor axon defects would become more severe when Smn protein was further reduced, 9 ng of MO was injected into embryos.

Table I. **Percentage of sides with at least one of the specified motor axon/nerve defects**

	Truncation		Branching	
	27 h	**36 h**	**27 h**	**36 h**
Control MO				
6 ng	3.5 ± 11.9[a]	0.0 ± 0.0	8.3 ± 7.3	0.0 ± 0.0
	n = 28[b]	*n* = 24	*n* = 24	*n* = 32
9 ng	5.6 ± 11.7	0.0 ± 0.0	14.3 ± 20.9	0.0 ± 0.0
	n = 18	*n* = 28	*n* = 14	*n* = 28
smn MO				
6 ng	35.3 ± 7.6[d]	61.5 ± 8.4[e]	23.6 ± 7.3[c]	44.6 ± 13.4[e]
	n = 156	*n* = 130	*n* = 140	*n* = 130
9 ng	13.6 ± 15.6	46.9 ± 12.4[e]	77.3 ± 17.5[e]	76.6 ± 10.5[e]
	n = 81	*n* = 128	*n* = 81	*n* = 128

Significance of control MO versus *smn* MO for each age, defect, and dose was determined by *t* test.
[a]Percentage of sides (±95% confidence interval).
[b]*n*, number of embryos.
[c]$P < 0.05$.
[d]$P < 0.0005$.
[e]$P < 0.0001$.

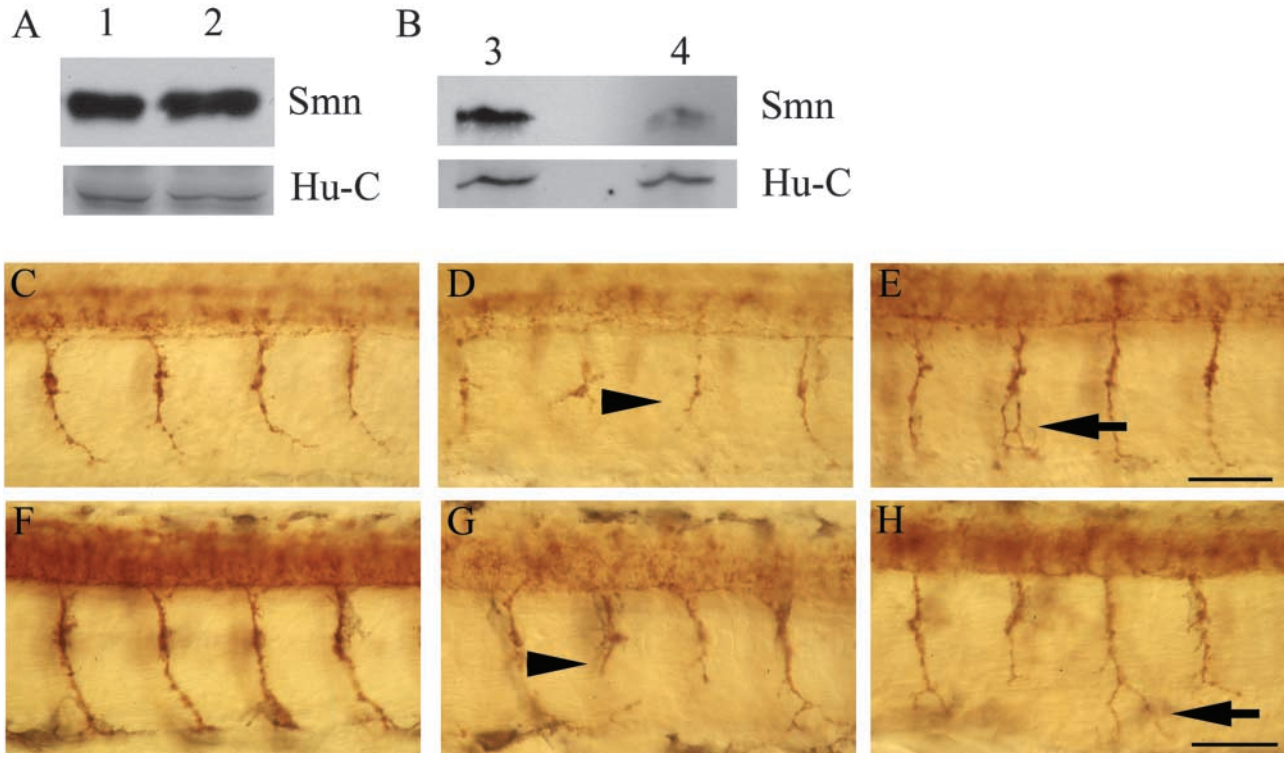

Figure 2. **Motor axons/nerves are abnormal in embryos injected with 9 ng of *smn* MO.** Western blot analysis of WT uninjected (lanes 1 and 3), control MO–injected (lane 2), and *smn* MO–injected (9 ng) (lane 4) embryos at 36 h. Hu-C, a neuronal marker, is shown as a loading control. Lateral views of whole-mount embryos labeled with znp1 mAb at 27 (C–E) and 36 h (F–H) in embryos injected with control MO (C and F) or *smn* MO (D, E, G, and H). Truncated motor axons/nerves (D and G; black arrowheads) and branched motor axons/nerves (E and H; black arrows) occur when Smn protein levels are further reduced. Bars: (C–E) 25 μm; (F–H) 30 μm.

Western blot analysis showed a 77% knockdown of protein (Fig. 2, A and B). In contrast to 89% survival when control MO was injected ($n = 164$), at this higher dose of *smn* MO, only 45% ($n = 433$) of the embryos survived, further suggesting the essentiality of Smn in zebrafish development.

Injecting higher doses of *smn* MO resulted in a dramatic increase in motor axon branching. At 27 h, 77.3% of sides from *smn* MO embryos had at least one branched motor axon (Table I; Fig. 2 E). The average number of motor axon branches per side was also increased at higher doses of MO (Table II). Branching defects were also significantly increased at 36 h; 76.6% of injected embryo sides had at least one branched motor nerve, compared with 44.6% of sides with the lower dose of *smn* MO (Table I; Fig. 2 H). These data indicate that the motor axon branching defect is more severe upon further knockdown of Smn.

Motor axon truncations were less evident at higher *smn* MO doses; in fact at 27 h, there is no significant difference when compared with control MO injections, where 5.6% of sides had truncated motor axons (Table I, Fig. 2 D). Also, all of the *smn* MO defective sides only had one truncated motor axon (Table II). At 36 h, a similar trend was apparent. 46.9% of 9 ng *smn* MO–injected embryo sides had at least one truncated motor nerve, which is slightly reduced compared with lower doses of MO (Table I; Fig. 2 G). The average number of truncated motor nerves per side is 2.47,

Table II. **Average number of the specified motor axon/nerve defects per affected side**

	Truncation		Branching	
	27 h	**36 h**	**27 h**	**36 h**
smn MO				
6 ng	1.89 ± 0.32[a]	2.81 ± 0.60	2.31 ± 0.39	2.50 ± 0.67
	$n = 156$[b]	$n = 130$	$n = 140$	$n = 130$
9 ng	1.00 ± 0.00	2.47 ± 0.57	5.13 ± 2.31[d]	5.26 ± 1.41[c]
	$n = 81$	$n = 128$	$n = 81$	$n = 128$

Significance was determined by a *t* test comparing each defect at 6 ng to the same defect at 9 ng.
[a]At 27 h, 10–12 znp1 mAb–labeled motor axons/nerves were scored per side; at 36 h, 14–16 motor axons/nerves were scored (±95% confidence interval).
[b]*n*, number of embryos.
[c]$P < 0.01$.
[d]$P < 0.0001$.

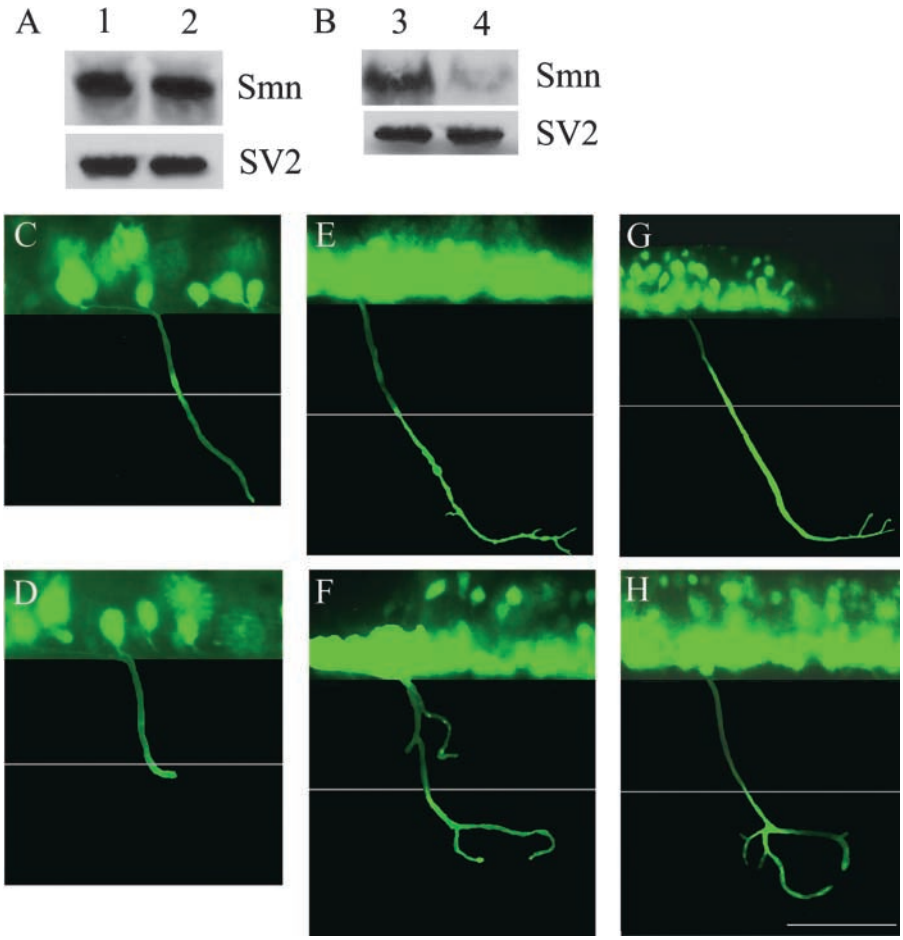

Figure 3. **Time-lapse imaging of defective motoneurons suggests that truncation defects precede branching defects.** Western blot analysis of WT uninjected (lanes 1 and 3), control MO–injected (lane 2), and *smn* MO–injected (9 ng) (lane 4) embryos at 74 h. Synaptic vesicle protein 2, SV2, is shown as a loading control. Lateral views of the medial pathway of a GFP-expressing motor nerve of a transgenic *gata2–GFP* embryo injected with either control MO (C, E, and G; $n = 10$) or *smn* MO (D, F, and H; $n = 13$). Ventral projecting motoneurons are shown at 36 (C and D), 50 (E and F), and 74 h (G and H). White lines demarcate the second intermediate target, the ventral aspect of the notochord. Only one GFP-expressing motor nerve was imaged, compiled, and placed on an artificial black background; the additional trunk nerves have been removed from the image. Bar, 50 μm.

slightly less than at lower doses of MO (Table II). These data suggest that further reduction of Smn protein levels results in more severe motor nerve branching defects and less severe truncation defects. To confirm that reduction in Smn results in motor axon/nerve defects, we used an additional, nonoverlapping *smn* MO and observed similar defects (Fig. S3, available at http://www.jcb.org/cgi/content/full/jcb.200303168/DC1), although this 5′ UTR MO was less efficient than the original MO described (Table SI, available at http://www.jcb.org/cgi/content/full/jcb.200303168/DC1).

Aberrant motor nerves remain defective over time

To determine the dynamics of the axon defects observed in *smn* MO–injected embryos, we analyzed motor nerves over several days using *gata2–GFP* transgenic zebrafish (Meng et al., 1997). In this transgenic line, secondary motoneuron cell bodies and ventrally projecting axons express GFP starting at ~33 h. 9 ng of *smn* MO or control MO was injected into *gata2–GFP* embryos, and ventral motor nerves were visualized from 36 to 74 h. *smn* MO was still effective in knocking down Smn protein at later time points, as evidenced by Western blot analysis performed at 74 h, which shows a 88% reduction in Smn protein (Fig. 3, A and B).

13 individual motor nerves were identified in *smn* MO–injected embryos ($n = 13$) at 36 h and were followed until 74 h. At 36 h, each of the 13 nerves was truncated at or near the ventral edge of the notochord (Fig. 3 D), a second intermediate target for motor axons (Beattie et al., 2000; Fig. S1). When the same motor nerves were examined at 52 h, 92% (12/13) of the nerves remained truncated but had be-

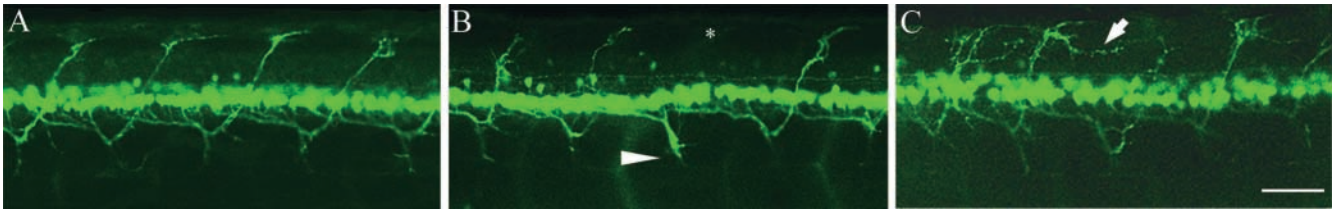

Figure 4. **Dorsally projecting motor nerves are also truncated and branched when Smn protein is decreased.** Lateral view of a confocal image of a GFP-expressing, dorsally projecting motor nerves in a transgenic *islet1–GFP* embryo injected with either 9 ng of control MO (A; $n = 50$) or *smn* MO (B and C; $n = 89$) at 74 h. White arrowhead and asterisk (B) denote a truncated nerve. White arrow (C) indicates a nerve branch extending into the adjacent hemisegment. Bar, 50 μm.

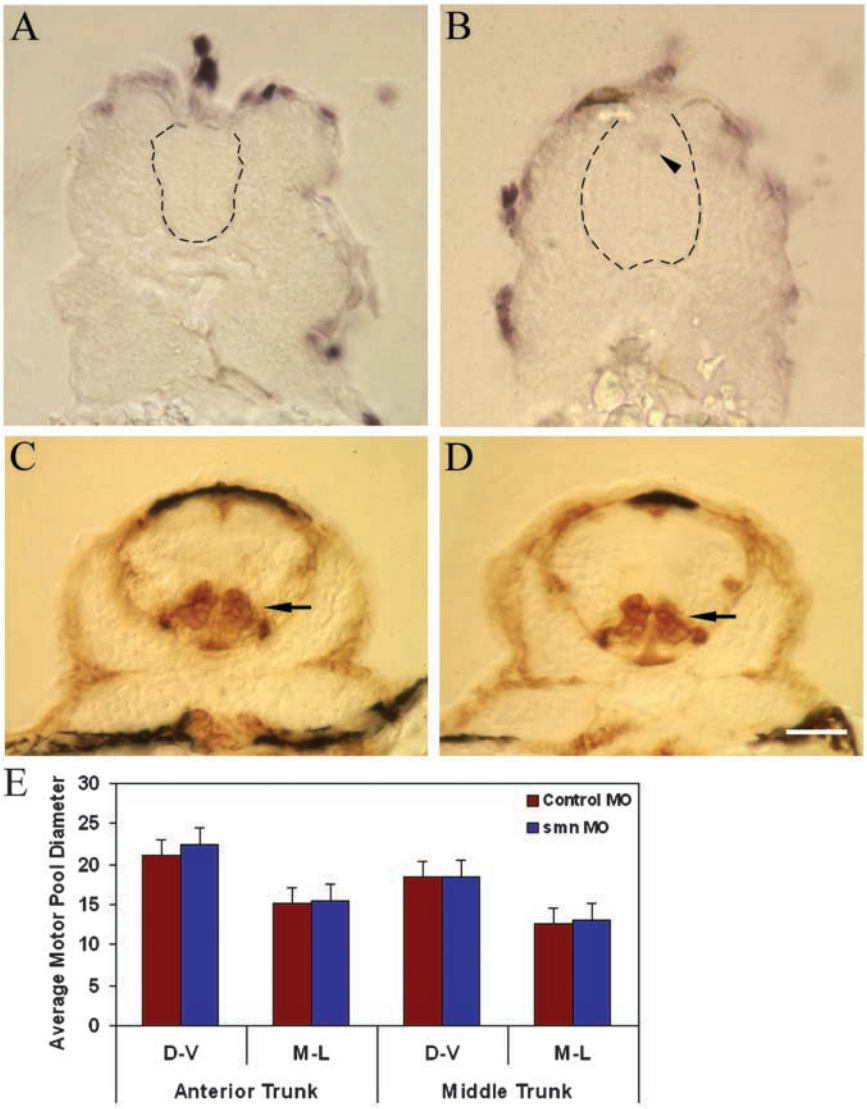

Figure 5. **Decreased levels of Smn do not initially result in motoneuron cell death.** Cross section view (dorsal to the top) of TUNEL-stained 50-h control MO–injected (A; $n = 3$) and *smn* MO–injected (9 ng) (B; $n = 15$) embryos. TUNEL-positive (purple) cells are present on the skin of both the *smn* MO– and control MO–injected embryos, which is not uncommon for this assay. Occasionally, (B) TUNEL-positive cells (black arrowhead) present in the dorsal spinal cord, corresponding to the sensory Rohon-Beard neurons (entire spinal cord demarcated by black dashed lines). Cross section view of zn-5 mAb–stained secondary motoneuron cell bodies (arrows) of 50-h control MO–injected (C; $n = 6$) and *smn* MO–injected (9 ng) (D; $n = 41$) embryos. (E) Motor pool diameter (μm) was measured on medial-lateral (M-L) and dorsal-ventral (D-V) axes (error bars indicate standard error). Anterior trunk was defined as hemisegments 1–5, whereas middle trunk was defined as hemisegments 6–14. *t* test concluded that $P > 0.1$ among motor pools of control MO– and *smn* MO–injected embryos. Bar, 25 μm.

gun to branch (Fig. 3 F). Upon examination at 76 h, 85% (11/13) of the nerves were truncated and branched (Fig. 3 H). The remaining motor nerves (2/13) that did reach the ventral muscle projected into the preceding hemisegment, nearly touching the motor nerve in the adjacent hemisegment; although these motor nerves were not truncated or branched, their pathfinding was clearly erroneous. In contrast, all of the nerves in control MO–injected embryos ($n = 10$) exhibited the stereotypic ventral nerve projections (Fig. 3, C, E, and G). These data show that defective motor nerves are dynamic, first becoming truncated and then branching at the site of truncation. Thus, nerve truncations are still occurring at higher doses of *smn* MO, but the extensive branching obscures this phenotype.

Knockdown of *smn* also causes aberrant dorsal projecting motor nerves

To determine whether other spinal motor axons were affected by decreased levels of Smn protein, we analyzed dorsal motor nerves in *islet1–GFP* transgenic zebrafish. Among other neuronal types, this transgenic line has GFP-expressing secondary motoneuron cell bodies and dorsally projecting axons (Fig. 4 A; Higashijima et al., 2000). 9 ng of *smn* MO or control MO was injected into *islet1–GFP* transgenic embryos, and dorsal nerves were analyzed at ~74 h. Like ventral motor nerves, dorsally projecting motor nerves exhibited truncation and branching defects as a result of *smn* knockdown (Fig. 4, B and C). Branching is also more prominent at higher doses of *smn* MO in these nerves. 69.1% ($n = 178$) of sides of *smn* MO–injected embryos had at least one branched dorsal projecting motor nerve, whereas control MO–injected embryos had only 8.0% of sides with a branched dorsal nerve ($n = 50$). In contrast, 32.6% ($n = 178$) of sides of *smn* MO–injected embryos had at least one truncated nerve, whereas control MO–injected embryos had no truncated dorsal projecting nerves ($n = 50$). These defects are consistent with those seen in ventral projecting motor nerves, suggesting that dorsal projecting motoneurons are also affected by reduction of Smn protein.

Human *SMN* mRNA partially rescues motor nerve defects

To confirm the specificity of the MO function, RNA rescue experiments were performed using human *SMN*

mRNA. One- to four-cell *gata2–GFP* embryos were injected with a mixture of *smn* MO (9 ng) and h*SMN* mRNA. When compared with *smn* MO alone, coinjection of h*SMN* and *smn* MO resulted in rescue of both the branching and truncation nerve defects (Table III). The partial rescue observed was probably due to the mosaic nature of the mRNA and MO injections, as reported by others (McClintock et al., 2002). The specificity of the RNA rescue was confirmed by the lack of rescue when h*SMNΔ7* mRNA, a common mutation and the major form of mRNA produced by *SMN2*, was coinjected with *smn* MO (Table III; Lefebvre et al., 1995). The percentage of sides with branched motor nerves is slightly reduced compared with MO alone, likely due to the slight activity of the hSMNΔ7 protein (Cifuentes-Diaz et al., 2002; unpublished data). These rescue experiments confirm that the motor nerve defects observed when *smn* MO is injected are a result of the reduction of Smn protein and further validate this system as a model for SMA.

Table III. **Percentage of sides with at least one of the specified motor nerve defects**

	Branching	Truncation
WT uninjected	19.4 ± 7.6[a]	3.7 ± 3.6
	n = 54[b]	*n* = 54
smn MO (9 ng)	63.9 ± 6.5	19.4 ± 5.4
	n = 108	*n* = 108
smn MO (9 ng) and h*SMN* RNA	37.1 ± 12.4[d]	8.1 ± 7.0[c]
	n = 31	*n* = 31
smn MO (9 ng) and h*SMNΔ7* RNA	56.0 ± 8.1	23.3 ± 7.0
	n = 75	*n* = 75

Significance of h*SMN* mRNA rescue versus *smn* MO alone for each defect was determined by *t* test.
[a]GFP-expressing motoneurons were scored at 52 h (±95% confidence interval).
[b]*n*, number of embryos.
[c]$P < 0.02$.
[d]$P < 0.0001$.

Motor axon defects are not caused by cell death

To determine whether the motor axon defects observed upon *smn* knockdown were caused by neuronal apoptosis, a TUNEL assay was performed. Unlike higher vertebrates, naturally occurring motoneuron cell death in the zebrafish ventral spinal cord has not been reported (Cole and Ross, 2001). Embryos were injected with 9 ng control MO or *smn* MO and then analyzed at 27 ($n = 10$), 36 ($n = 10$), and 50 h ($n = 15$). None of the injected embryos had any TUNEL-positive cells in the ventral spinal cord (Fig. 5, A and B). TUNEL-positive cells could occasionally be seen in the dorsal spinal cord, corresponding to the Rohon-Beard sensory neurons (Fig. 5 B; arrowhead), which have previously been shown to undergo apoptosis at this age (Cole and Ross, 2001). To further confirm that motoneuron numbers were not reduced by means other than apoptosis, the diameter of the spinal motor pool was measured. Embryos injected with control or *smn* MO were labeled with anti-neurolin mAb (zn-5), which labels the cell surface of secondary motoneurons in the spinal cord (Fashena and Westerfield, 1999). To analyze the motor pool size, the diameter was measured both dorso-ventrally and medio-laterally on both sides of the midline (Fig. 5, C and D). There was no significant difference in motor pool diameter on either axis between control MO– and *smn* MO–injected embryos (Fig. 5 E). These data indicate that the motor axon defects observed upon Smn reduction are not caused by motoneuron death and further support the idea that Smn is needed for motor axon development.

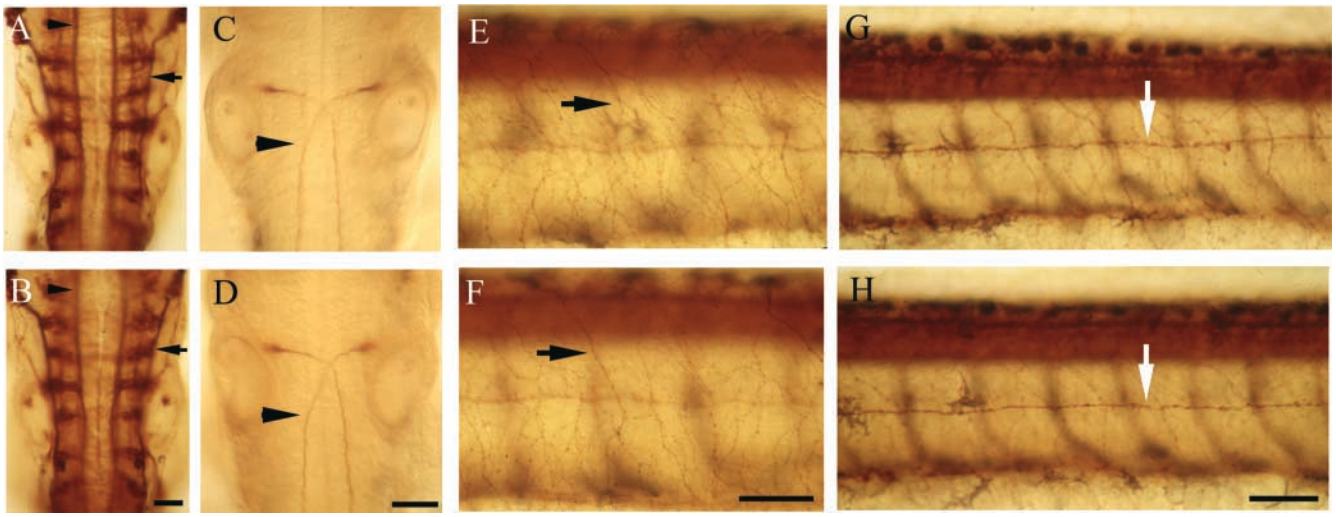

Figure 6. **Other neurons and axon tracts are unaffected upon knockdown of Smn protein.** Dorsal view (anterior to the top) of the hindbrain stained with acetylated tubulin mAb in 27-h control MO–injected (A; $n = 40$) and *smn* MO–injected (9 ng) (B; $n = 39$) embryos showing the medial longitudinal fascicle (black arrowheads) and the lateral longitudinal fascicle (black arrows). Dorsal view of the hindbrain Mauthner neuron cell body and axon (arrowhead) stained with 3A10 mAb in 34-h control MO–injected (C; $n = 61$) and *smn* MO–injected (D; $n = 32$) embryos. Lateral views of (E and F) Rohon-Beard (black arrow) and (G and H) lateral line sensory neurons (white arrow) stained with acetylated tubulin mAb in 34-h control MO–injected (E and G; $n = 40$) and *smn* MO–injected (F and H; $n = 39$) embryos. Bars: (A and B) 50 μm; (C and D) 40 μm; (E–H) 50 μm.

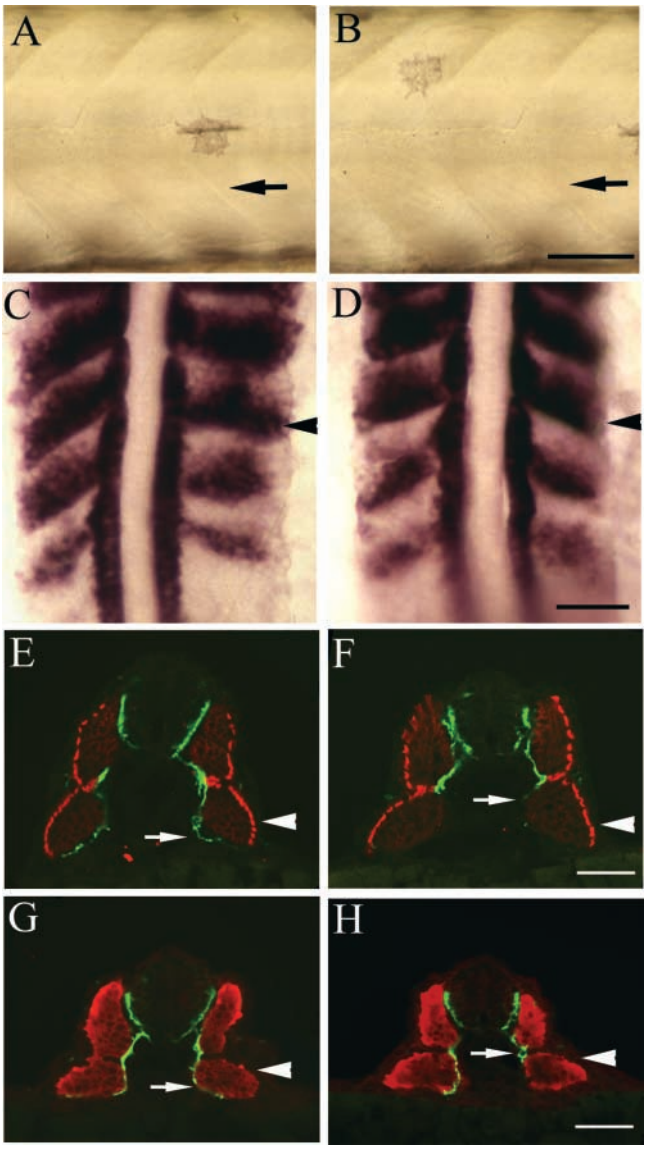

Figure 7. **Muscle development is normal when Smn is decreased.** Nomarski lateral views of mid-trunk muscle from 50-h *gata2–GFP* transgenic embryos injected with 9 ng of control MO (A; $n = 20$) or *smn* MO (B; $n = 20$) showing somitic boundaries (black arrows). Dorsal views of 22-h whole-mount in situ hybridization of *myoD* (purple; black arrowhead) in control MO–injected (C; $n = 31$) and *smn* MO–injected (D; $n = 18$) embryos. Cross section of 27-h znp1 (motor axon; arrows) and F59 (slow muscle; arrowheads) mAb–stained embryos injected with control MO (E; $n = 40$) or *smn* MO (F; $n = 65$). Cross section of 27-h znp1 (motor axon; arrows) and F310 (fast muscle; arrowheads) mAb–stained embryos injected with control MO (G; $n = 20$) or *smn* MO (H; $n = 41$). Bars: (A–D) 75 μm; (E–H) 30 μm.

Other neuronal cell types and axon tracts are not affected by Smn knockdown

In human and mouse models of SMA, the affect of decreased levels of SMN is specific for motoneurons. To determine if the defects resulting from Smn knockdown were also motoneuron specific, we examined populations of interneurons and sensory neurons using the acetylated tubulin mAb. Many zebrafish hindbrain interneurons have stereotyped axonal projections that extend into the spinal cord (Mendelson, 1986; Metcalfe et al., 1986). We saw no defects in the medial longitudinal fascicle or the lateral longitudinal fascicle, both of which contain hindbrain and midbrain axons descending into the spinal cord (Fig. 6, A and B). To look for more subtle defects, we examined the single commissural axon of the Mauthner neuron present in hindbrain rhombomere 4. Using the 3A10 mAb, we found that in *smn* MO–injected embryos, the Mauthner axon projected across the midline and down the spinal cord in a manner indistinguishable from control MO–injected embryos (Fig. 6, C and D). Rohon-Beard sensory neurons, present in the dorsal spinal cord (Lamborghini, 1980; Metcalfe et al., 1990), send axons into the peripheral muscle and skin. These cells and their axons were also unaffected by Smn knockdown (Fig. 6, E and F). Lastly, we looked at the lateral line, a group of sensory neurons that send axons the length of the developing embryo. We observed no difference in length or morphology of the lateral line axons in control MO– or *smn* MO–injected embryos (Fig. 6, H and G). Thus, interneurons and sensory neurons are unaffected by decreased levels of Smn protein and support the finding that motoneurons are uniquely sensitive to decreased Smn levels.

Smn knockdown does not affect muscle development

To determine whether the motor axon defects observed were due to defects in muscle development, we examined the development and patterning of the myotomes. Overall myotome morphology was analyzed using live *gata2–GFP* transgenic embryos injected with either control MO or *smn* MO. Nomarski images were taken of muscle segments containing defective GFP-expressing nerves. No difference was seen in the muscle morphology between control MO– and *smn* MO–injected embryos (Fig. 7, A and B). No defects were seen in early muscle patterning in *smn* MO–injected embryos compared with control MO, as assayed by *myoD* expression, a gene expressed in the posterior region of the developing somite (Weinberg et al., 1996; Fig. 7, C and D). Lastly, we asked whether muscle cells were correctly specified by characterizing slow and fast muscle in *smn* MO–injected embryos. Using the slow muscle mAb F59 (Crow and Stockdale, 1986; Devoto et al., 1996) and the fast muscle mAb F310 (Crow and Stockdale, 1986; Zeller et al., 2002), we found no difference between muscle specification and organization upon depletion of Smn (Fig. 7, E–H). These data suggest that low levels of Smn do not adversely affect muscle organization, specification, or development.

As motor axons in *smn* MO embryos displayed aberrant axon outgrowth, we asked whether these axons were still capable of forming synapses on the muscle fibers. To address this, we analyzed acetylcholine receptor (AChR) clusters in *smn* MO embryos at 3 d. Using rhodamine-conjugated α-bungarotoxin, we found that all axons in *smn* MO and control MO embryos colocalized with AChR clusters (Fig. 8, A–F), suggesting that the axons are innervating muscle fibers but lack the stereotyped pattern of innervation (Fig. 8, D–F, arrows). Consistent with this observation, we found no overt movement defects or paralysis in these embryos (unpublished data).

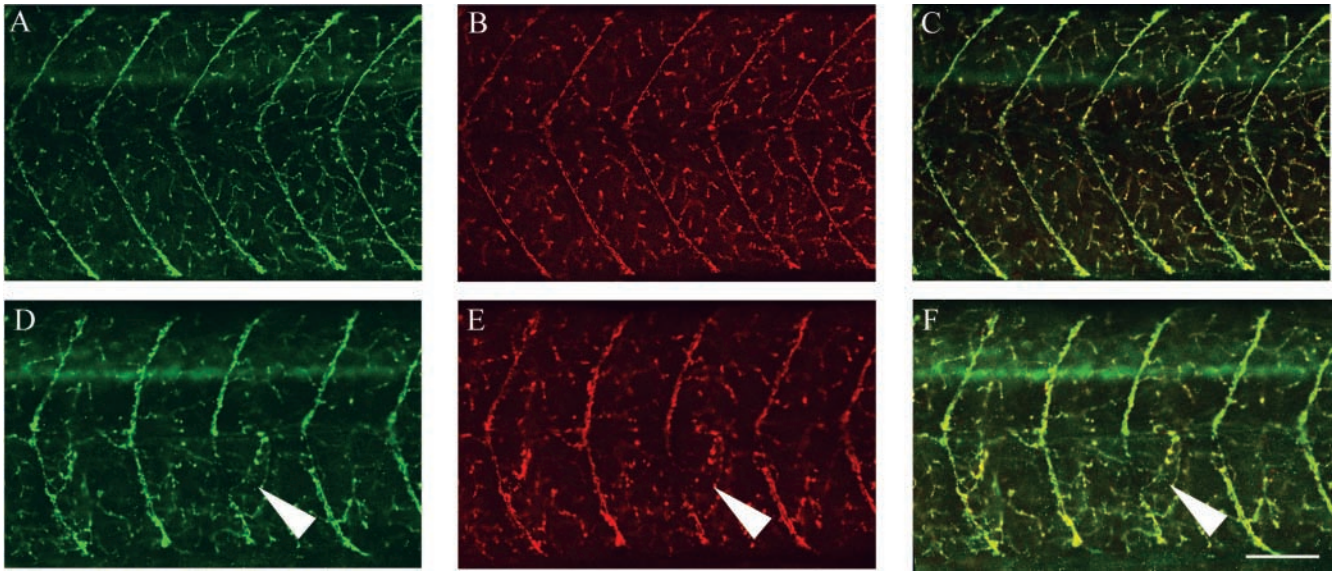

Figure 8. **AChR clustering is normal when Smn is decreased.** Lateral views of znp1 (A and D; motor axons, green) mAb, α-bungarotoxin (B and E; AChR, red) stained, and merge (C and F; yellow) 74-h larvae injected with control MO (A–C; $n = 18$) or *smn* MO (D–F; $n = 49$). Aberrant motor nerve (arrowhead) retains ability to cluster AChR. Bar, 50 μm.

Smn is acting cell autonomously in motoneurons

As Smn is expressed in all tissues, it is not clear where its function is required for normal motor axon development. To test whether Smn functions cell autonomously with respect to motoneurons, we reduced Smn levels in single motoneurons in otherwise WT embryos. Optical clarity of zebrafish embryos allows us to identify single primary motoneurons in living embryos and iontophorese these cells with vital fluorescent dyes (Eisen et al., 1989; Beattie et al., 2000). *smn* or control MO was iontophoresed with rhodamine dextran dye into CaP cell bodies at 19.5–20.5 h; CaP axons were then imaged at 43 h. 100 and 50 μM solutions were found to cause significant cell death when iontophoresed into motoneurons, whereas a solution containing 1 μM of *smn* MO only caused 45.5% of the CaP motoneurons to die.

CaP motoneurons iontophoresed with 1 μM control MO exhibited no axon defects ($n = 10$; Fig. 9 A). In contrast, CaP motoneurons, iontophoresed with *smn* MO when their growth cones were at the first intermediate target, were defective 76.9% of the time ($n = 13$; Fig. 9, B, C, and D). The defects observed, axon truncations and branches, were consistent with defects seen when the entire embryo was injected with *smn* MO. CaP motoneurons were also iontophoresed with *smn* MO when their growth cones were further ventral at the second intermediate target. Only 62.5% of these motor axons ($n = 8$; Fig. 9 D) were defective, suggesting that the longer the Smn protein is reduced

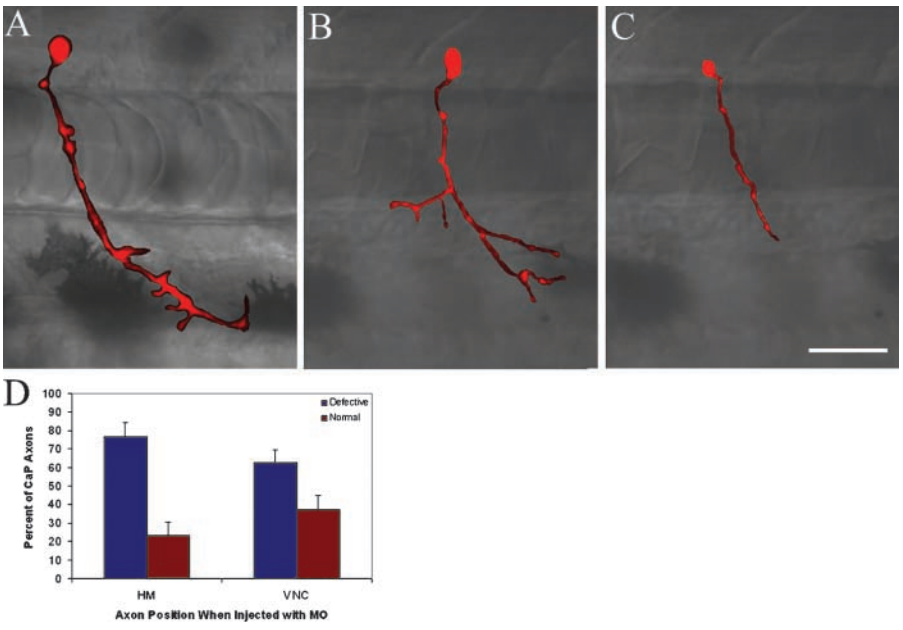

Figure 9. **Smn is acting cell autonomously in CaP motoneurons.** Lateral views of psuedocolor images of live CaP motoneurons directly iontophoresed with rhodamine dextran and control MO (A; $n = 10$) or *smn* MO (B and C; $n = 21$) visualized and imaged at 43 h. CaP motoneurons iontophoresed with *smn* MO exhibit axon branching (B) and truncation (C). (D) Percentage of *smn* MO–injected CaP motoneurons with defective and normal axons quantitated (error bars represent standard error). HM, nascent horizontal myoseptum; VNC, myotome adjacent to the ventral edge of the notochord. Bar, 50 μm.

during outgrowth, the more likely pathfinding errors, such as truncations and branches, will occur. The incomplete penetrance of these defects may suggest variability in the phenotype, as is seen when the entire embryo is injected with *smn* MO.

To show the specificity of these defects, *smn* MO and fluorescent rhodamine dextran were also iontophoresed into ventral longitudinal descending (VeLD) neurons, spinal interneurons with axons that descend into the tail region by 43 h (Kuwada et al., 1990; Hale et al., 2001). All VeLD interneurons iontophoresed with *smn* MO ($n = 4$) had axons that traveled into the tail region and showed no other defects, such as branching (unpublished data). This further indicates that knockdown of Smn protein causes motoneuron-specific defects. Taken together, these data show that Smn functions cell autonomously in motoneurons and plays a critical and specific role in motor axon outgrowth and pathfinding.

Discussion

Taking advantage of the relatively simple neuromuscular organization of the zebrafish embryo, we have shown that Smn has an essential function in motor axon development. The defects observed in motor axons upon knocking down Smn are independent of cell death and are specific for motoneurons. The data we present indicate that the earliest defects in SMA are in the developing motor axons and suggest that this defect in axon outgrowth and pathfinding may eventually lead to motoneuron death and SMA.

The motor axon defect in *smn* knockdown embryos

Embryos with decreased Smn levels show defects in motor axon outgrowth and pathfinding during the first three days of development. Defects were rarely seen in the proximal axon extending from the spinal cord to the first intermediate target, suggesting that initiation of axon outgrowth and pathfinding along the common pathway are unaffected by low Smn levels. Secondary motoneurons also displayed branching and truncation defects that continued up to 3 d. As primary and secondary motor axons fasciculate to form nerves, we cannot be certain that the defects observed at 36–72 h are defasciculation of the nerve or true branching of the axons. As branching in single CaP axons is seen, this suggests that true branching does occur. Although the motor axon projections are aberrant, these axons still colocalized with AChR, indicating that functional synapses had formed.

The motor axon branching and truncation defects were initially discovered upon injection of 6 ng of *smn* MO into zebrafish embryos. When a higher dose of MO, 9 ng, was used, there was a significant increase in the amount of motor axon branching and an apparent decrease in truncations. Analysis of embryos with GFP-expressing motor nerves, however, revealed that truncations were still occurring but were followed by branching, thus obscuring the truncation phenotype. These data indicate that the less Smn protein translated within the neuron, the greater the likelihood that the axon will branch. Ventral nerve truncations were consistently occurring at the second intermediate target. It is believed that intermediate targets are important for growth cones to proceed to their final targets (Tessier-Lavigne and Goodman, 1996). It is possible that in the presence of low Smn, growth cones stall at these locations, suggesting that they still try to assimilate cues. At very low levels of Smn, the growth cone may not even be responding to the intermediate target and branches indiscriminately.

Cell autonomy of Smn

Due to the distribution of SMN protein, it has been difficult to conclusively determine whether the primary defect resides in motoneurons or muscle. In *smn* MO–injected zebrafish embryos, the motoneurons are defective, but muscle specification, early patterning, and muscle development are normal, indicating that decreasing Smn is critical in motoneurons. We specifically reduced Smn in single motoneurons without affecting Smn levels in other neurons or muscle. Exclusively decreasing Smn in motoneurons recapitulated the motor axon defect seen when Smn was decreased throughout the embryo, indicating that Smn functions cell autonomously. We cannot, however, rule out the possibility that Smn also functions in muscle to affect motor axons.

Smn and motor axons

Recent mouse and human studies suggest that motor axons may be affected before motoneuron loss. Mice exhibiting neuronal depletion of SMN (Smn^{F7}/Smn^{D7}, NSE-Cre^{+}) exhibited a dramatic decrease in motor axons but only a modest decrease in motoneuron cell bodies at postnatal day 15 (Cifuentes-Diaz et al., 2002). Due to the severe reduction in full-length SMN and the relatively late developmental timing of this reduction, however, it is difficult to determine the disease relevance of these defects. Severe SMA mice ($Smn^{-/-}$ with one to two copies of *SMN2*; Hsieh-Li et al., 2000; Monani et al., 2000) show moderate motoneuron cell body loss, whereas mild SMA mice (A2G missense) show no motoneuron cell body loss several days after birth; mild SMA mice do, however, exhibit a mild reduction in both motoneuron cell bodies and motor axon roots at 3.5 mo (Monani et al., 2003). Motor unit number estimation (MUNE) studies in humans show that presymptomatic individuals exhibit high motoneuron counts that dramatically decrease with onset of the disease (Bromberg and Swoboda, 2002). These results indicate that motoneuron cell body loss is a late feature of the disease. Our data are consistent with these findings and support the idea that axons are affected before cell death.

SMN has also been shown to localize in developing motoneurons. Rat SMN colocalizes with cytoskeletal elements in the spinal motor axons during nervous system maturation (Pagliardini et al., 2000). In primary motoneuron cultures from E14 mice embryos, SMN is enriched in branch points and growth cones (Jablonka et al., 2001). SMN has also been found in growth cones of P19 neurons (Fan and Simard, 2002). Interestingly, SMN interacting protein 1 (SIP1), a protein important in spliceosomal snRNP biogenesis (Fischer et al., 1997), does not coenrich in axon branch points, indicating the possibility of a unique SMN complex and function at these locations (Jablonka et al., 2001). Taken together with our findings of abnormal motor axon branching when Smn is depleted, the data suggest that Smn

plays an important function in motor axon development and maintenance.

Although a mechanism by which SMN functions in motoneuron development remains unclear, recent data do give clues. SMN has been shown to interact with profilin (Giesemann et al., 1999), a protein involved in actin polymerization and growth cone motility (Gutsche-Perelroizen et al., 1999; Wills et al., 1999; Kim et al., 2001), processes important for axon outgrowth. Data have also implicated an interaction between SMN and motoneuron-enriched RNA processing molecules, hn-RNP-Q and hn-RNP-R (Rossoll et al., 2002). These proteins play a role in RNA transport, editing, and translation. RNA transport into the axon followed by localized protein translation has been shown to be important for growth cones to proceed past intermediate targets (Brittis et al., 2002). It is possible that SMN in axons and growth cones may be associated with RNP complex assembly associated with transport and/or translation of mRNA. Recent experiments have shown that SMN localizes with cytoskeletal filaments and is actively transported down axons (Zhang et al., 2003), further indicating that SMN may be involved in transport and the resulting translation of important axon guidance cues. It is possible that if SMN is reduced, motor axons cannot respond to cues at intermediate targets by turning on local translation, resulting in axon defects. Our finding that GFP-expressing motor nerves in *smn* MO–injected embryos are truncated at the second intermediate target is consistent with this idea. The validity of this model, however, will depend on elucidating a direct relationship between Smn and localized protein translation machinery in motor axon growth cones.

Materials and methods

Fish maintenance

Adult zebrafish and embryos were maintained as previously described (Westerfield, 1995), allowed to develop at ~28.5°C, and staged by hours or days after fertilization (Kimmel et al., 1995). All fish used in this study were on the *AB background unless otherwise specified.

Nomenclature

Consistent with guidelines for different species, the mouse, human, or rat protein is SMN and the gene is *SMN* (human) or *Smn* (mouse). In fish, the protein is Smn, and the gene is *smn* (http://zfin.org/zf_info/nomen.html).

Physical mapping and southern blot analysis

Zebrafish *smn* primers (5′-GTGATGATTCTGACATTTGG-3′ and 5′-CCATCCTCACCTTTCAAAGC-3′) were used to map the gene on the LN54 radiation hybrid panel (Hukriede et al., 1999). *smn* maps to linkage group 5, 3.25 cM from marker fb39c12. Southern blots were performed as previously described (Monani et al., 2000). The *smn* probe was generated by PCR with the following primer sequences: 5′-GTGATGATTCTGACATTTGG-3′ and 5′-GTCTTCAGAGCATCTTCATCC-3′. The zebrafish *islet2* gene was used as a control.

Whole-mount in situ hybridization

Zebrafish *smn* cDNA clone (GenBank/EMBL/DDBJ accession nos. Y17256, AA494875, AA494767, and AF083557) was used to make sense and antisense digoxigenin-labeled riboprobes of 1016 bp (Bertrandy et al., 1999). The sense (Sp6) and antisense (T7) *smn* riboprobes were synthesized from plasmid linearized with XhoI and HindIII, respectively. *Islet2* and *MyoD* riboprobes were synthesized as previously described (Appel et al., 1995; Weinberg et al., 1996). Whole-mount in situ hybridization protocol (1277073; Roche) was performed as previously described (Thisse et al., 1993).

Antisense MO and synthetic mRNA injections

An antisense MO was designed against the 5′ start sequence of the *smn* gene (Gene Tools, Inc.); 5′-CGACATCTTCTGCACCATTGGC-3′. An additional nonoverlapping MO was also designed ~20 bp upstream of the original MO (designated 5′ UTR MO); 5′-TTTAAATATTTCCCAAGTCCAACGT-3′. Two- to four-cell *AB, *gata2–GFP* (Meng et al., 1997), or *islet1–GFP* (Higashijima et al., 2000) embryos were injected with ~6 or 9 ng of MO in Danieau's solution with phenol red dye according to protocol (Nasevicius and Ekker, 2000). A standard control (Gene Tools, Inc.) MO (5′-CCTCTTACCTCAGTTACAATTTATA-3′) was used at 6 or 9 ng for control injections. Synthetic capped human SMN mRNA was produced using mMESSAGE mMACHINE kit (Ambion) according to the manufacturer's instructions. mRNA was produced from previously described plasmids (Le et al., 2000) linearized with Xho1. Approximately 300–500 pg of mRNA was coinjected with 9 ng of *smn* MO.

Immunohistochemistry

Immunohistochemistry and imaging were performed essentially as previously described (Beattie et al., 2000). The following mAbs were used: znp1 (1:100; Melancon et al., 1997), anti–acetylated tubulin (1:250; T-6793; Sigma-Aldrich), anti–slow twitch myosin F59 (1:10; Crow and Stockdale, 1986; Devoto et al., 1996), anti–fast twitch myosin F310 (1:10; Crow and Stockdale, 1986; Zeller et al., 2002), 3A10 (1:10; Hatta, 1992), and anti–neurolin zn-5 (1:75; Fashena and Westerfield, 1999). FITC (IgG2A) and TRITC (IgG1) isotype-specific conjugate secondary Abs (1080–02 and 1070–03, respectively; Southern Biotechnology Associates, Inc.) were used for fluorescent detection of znp-1 (IgG2A) and F59/F310 (IgG1) mAbs. Cross-sectional analysis was performed by embedding embryos in 1.5% agar/5% sucrose and sectioning on a cryostat at 16 μm. All immunofluorescent images were analyzed using a confocal microscope and photographed using digital imagery (Nikon Optiphot 2; Bio-Rad Laboratories, Inc. MRC 1024) unless otherwise specified.

Western blot analysis

MO-injected embryos were manually dechorionated and deyolked in a slurry of physiologic Ringers (Westerfield, 1995), Ringers ice chips, and protease inhibitors (Complete Mini; 1836170; Roche). Deyolked embryo samples were prepared and Western blots were performed as previously described (Monani et al., 2003). Smn (1:1,000; MANSMA7 or MANSMA21; Young et al., 2000b), anti–synaptic vesicle (SV2) protein (1:200; Buckley and Kelly, 1985), and anti–Hu 16A11 (1:500; A-21271; Molecular Probes; Marusich et al., 1994) mAb were visualized using the ECL Detection Kit (RPN 2109; Amersham Biosciences). Quantification of bands was performed using a densitometer (Shimadzu, Inc.).

Visualization of GFP transgenic zebrafish

Live *gata2–GFP* MO-injected transgenic zebrafish (Meng et al., 1997) were anesthetized in tricaine (A-5040; Sigma-Aldrich) at 36, 52, and 74 h and mounted on a glass coverslip. Individual motor nerves were visualized and imaged using a Photometrics SPOT camera. Images were compiled and edited using Adobe Photoshop® software. MO-injected *islet1*–GFP embryos (Higashijima et al., 2000) were fixed at 72 h in 4% paraformaldehyde for 2 h at room temperature.

TUNEL assay

TUNEL assay was performed according to the manufacturer's protocol on staged embryos (Cole and Ross, 2001). Digoxigenin-labeled dUTP was used to label fragmenting DNA ends (Terminal Transferase Assay; 220582; Roche), and then embryos were sectioned on a cryostat at 16 μm.

Detection of neuromuscular junctions

MO-injected embryos were staged and fixed in 4% paraformaldehyde for 2 h at room temperature and water soaked for 3–6 h. After collagenase (C-9891; Sigma-Aldrich) treatment, embryos were then incubated in Alexa®594-conjugated α-bungarotoxin (10 μg/ml; B13423; Molecular Probes) for 30 min, essentially as previously described (Ono et al., 2001). Embryos were then Ab stained using znp-1 and a FITC-conjugated secondary Ab.

Single cell knockdown of *smn*

Glass capillary microelectrodes were backfilled with a solution containing 2.5% rhodamine dextran (3,000 MW; Molecular Probes) and *smn* or control MO. 19.5–20.5-h embryos were anesthetized in tricaine and mounted in agar on a microslide as previously described (Eisen et al., 1989; Beattie et al., 2000). Individual CaP motoneurons or VeLD interneurons were im-

paled electrically by oscillating the electrode tip as previously described (Eisen et al., 1989). Solution was added to the cell by iontophoresis. Images were taken with a Photometrics SPOT camera and compiled and edited in Adobe Photoshop®.

Online supplemental material

The supplemental material is available at http://www.jcb.org/cgi/content/full/jcb.200303168/DC1. Fig. S1 diagrams primary and secondary motor axon pathfinding in the developing zebrafish. Fig. S2 shows the expression pattern of *smn* during the development of zebrafish. Fig. S3 shows that an additional 5′ UTR *smn* MO results in similar motor axon defects. Table SI shows the percentage of sides with motor axon/nerve defects using additional 5′ UTR *smn* MO.

We thank Shuo Lin (University of California, Los Angeles, CA) and Michael Granato (University of Pennsylvania, Philadelphia, PA) for *gata2–GFP* fish; Hitoshi Okamoto (RIKEN Brain Science Institute, Saitama, Japan), Shin-ichi Higashijima (State University of New York at Stony Brook, Stony Brook, NY), and Anad Chandrasekhar (University of Missouri, Columbia, MO) for *islet1–GFP* fish; Frank Stockdale (Stanford University, Stanford, CA) for F59 and F310 mAb; Thanh Le (The Ohio State University) for *SMN* constructs; and Jiyan Ma for critical reading of the manuscript. The 3A10 mAb, developed by Thomas M. Jessell and Jane Dodd, and the SV2 mAb, developed by Kathleen M. Buckley, were obtained from the Developmental Studies Hybridoma Bank developed under the auspices of the National Institute of Child Health and Human Development and maintained by The University of Iowa Department of Biological Sciences.

U.R. Monani is the recipient of a Development Grant from the Muscular Dystrophy Association of America. This research is supported by National Institutes of Health grant RO1NS41649.

Submitted: 26 March 2003
Accepted: 14 July 2003

References

Appel, B., V. Korzh, E. Glasgow, S. Thor, T. Edlund, I.B. Dawid, and J.S. Eisen. 1995. Motoneuron fate specification revealed by patterned LIM homeobox gene expression in embryonic zebrafish. *Development.* 121:4117–4125.

Beattie, C.E. 2000. Control of motor axon guidance in the zebrafish embryo. *Brain Res. Bull.* 53:489–500.

Beattie, C.E., E. Melancon, and J.S. Eisen. 2000. Mutations in the stumpy gene define intermediate targets for zebrafish motor axons. *Development.* 127: 2653–2662.

Bertrandy, S., P. Burlet, O. Clermont, C. Huber, C. Fondrat, D. Thierry-Mieg, A. Munnich, and S. Lefebvre. 1999. The RNA-binding properties of SMN: deletion analysis of the zebrafish orthologue defines domains conserved in evolution. *Hum. Mol. Genet.* 8:775–782.

Brittis, P.A., Q. Lu, and J.G. Flanagan. 2002. Axonal protein synthesis provides a mechanism for localized regulation at an intermediate target. *Cell.* 110:223–235.

Bromberg, M.B., and K.J. Swoboda. 2002. Motor unit number estimation in infants and children with spinal muscular atrophy. *Muscle Nerve.* 25:445–447.

Buckley, K.M., and R.B. Kelly. 1985. Identification of a transmembrane glycoprotein specific for secretory vesicles of neurons and endocrine cells. *J. Cell. Biol.* 100:1284–1294.

Cartegni, L., and A.R. Krainer. 2002. Disruption of an SF2/ASF-dependent exonic splicing enhancer in SMN2 causes spinal muscular atrophy in the absence of SMN1. *Nat. Genet.* 30:377–384.

Cifuentes-Diaz, C., S. Nicole, M.E. Velasco, C. Borra-Cebrian, C. Panozzo, T. Frugier, G. Millet, N. Roblot, V. Joshi, and J. Melki. 2002. Neurofilament accumulation at the motor endplate and lack of axonal sprouting in a spinal muscular atrophy mouse model. *Hum. Mol. Genet.* 11:1439–1447.

Cole, L.K., and L.D. Ross. 2001. Apoptosis in the developing zebrafish embryo. *Dev. Biol.* 240:123–142.

Coovert, D.D., T.T. Le, P.E. McAndrew, J. Strasswimmer, T.O. Crawford, J.R. Mendell, S.E. Coulson, E.J. Androphy, T.W. Prior, and A.H. Burghes. 1997. The survival motor neuron protein in spinal muscular atrophy. *Hum. Mol. Genet.* 6:1205–1214.

Crawford, T.O., and C.A. Pardo. 1996. The neurobiology of childhood spinal muscular atrophy. *Neurobiol. Dis.* 3:97–110.

Crow, M.T., and F.E. Stockdale. 1986. Myosin expression and specialization among the earliest muscle fibers of the developing avian limb. *Dev. Biol.* 113:238–254.

Devoto, S.H., E. Melancon, J.S. Eisen, and M. Westerfield. 1996. Identification of separate slow and fast muscle precursor cells in vivo, prior to somite formation. *Development.* 122:3371–3380.

DiDonato, C.J., X.N. Chen, D. Noya, J.R. Korenberg, J.H. Nadeau, and L.R. Simard. 1997. Cloning, characterization, and copy number of the murine survival motor neuron gene: homolog of the spinal muscular atrophy-determining gene. *Genome Res.* 7:339–352.

Dodd, A., P.M. Curtis, L.C. Williams, and D.R. Love. 2000. Zebrafish: bridging the gap between development and disease. *Hum. Mol. Genet.* 9:2443–2449.

Eisen, J.S., P.Z. Myers, and M. Westerfield. 1986. Pathway selection by growth cones of identified motoneurones in live zebra fish embryos. *Nature.* 320: 269–271.

Eisen, J.S., S.H. Pike, and B. Debu. 1989. The growth cones of identified motoneurons in embryonic zebrafish select appropriate pathways in the absence of specific cellular interactions. *Neuron.* 2:1097–1104.

Fan, L., and L.R. Simard. 2002. Survival motor neuron (SMN) protein: role in neurite outgrowth and neuromuscular maturation during neuronal differentiation and development. *Hum. Mol. Genet.* 11:1605–1614.

Fashena, D., and M. Westerfield. 1999. Secondary motoneuron axons localize DM-GRASP on their fasciculated segments. *J. Comp. Neurol.* 406:415–424.

Fischer, U., Q. Liu, and G. Dreyfuss. 1997. The SMN-SIP1 complex has an essential role in spliceosomal snRNP biogenesis. *Cell.* 90:1023–1029.

Giesemann, T., S. Rathke-Hartlieb, M. Rothkegel, J.W. Bartsch, S. Buchmeier, B.M. Jockusch, and H. Jockusch. 1999. A role for polyproline motifs in the spinal muscular atrophy protein SMN. Profilins bind to and colocalize with smn in nuclear gems. *J. Biol. Chem.* 274:37908–37914.

Grunwald, D.J., and J.S. Eisen. 2002. Headwaters of the zebrafish-emergence of a new model vertebrate. *Nat. Rev. Genet.* 3:717–724.

Gutsche-Perelroizen, I., J. Lepault, A. Ott, and M.F. Carlier. 1999. Filament assembly from profilin-actin. *J. Biol. Chem.* 274:6234–6243.

Hale, M.E., D.A. Ritter, and J.R. Fetcho. 2001. A confocal study of spinal interneurons in living larval zebrafish. *J. Comp. Neurol.* 437:1–16.

Hatta, K. 1992. Role of the floor plate in axonal patterning in the zebrafish CNS. *Neuron.* 9:629–642.

Higashijima, S., Y. Hotta, and H. Okamoto. 2000. Visualization of cranial motor neurons in live transgenic zebrafish expressing green fluorescent protein under the control of the islet-1 promoter/enhancer. *J. Neurosci.* 20:206–218.

Hsieh-Li, H.M., J.G. Chang, Y.J. Jong, M.H. Wu, N.M. Wang, C.H. Tsai, and H. Li. 2000. A mouse model for spinal muscular atrophy. *Nat. Genet.* 24: 66–70.

Hukriede, N.A., L. Joly, M. Tsang, J. Miles, P. Tellis, J.A. Epstein, W.B. Barbazuk, F.N. Li, B. Paw, J.H. Postlethwait, et al. 1999. Radiation hybrid mapping of the zebrafish genome. *Proc. Natl. Acad. Sci. USA.* 96:9745–9750.

Jablonka, S., M. Bandilla, S. Wiese, D. Buhler, B. Wirth, M. Sendtner, and U. Fischer. 2001. Co-regulation of survival of motor neuron (SMN) protein and its interactor SIP1 during development and in spinal muscular atrophy. *Hum. Mol. Genet.* 10:497–505.

Kim, Y.S., S. Furman, H. Sink, and M.F. VanBerkum. 2001. Calmodulin and profilin coregulate axon outgrowth in *Drosophila*. *J. Neurobiol.* 47:26–38.

Kimmel, C.B., W.W. Ballard, S.R. Kimmel, B. Ullmann, and T.F. Schilling. 1995. Stages of embryonic development of the zebrafish. *Dev. Dyn.* 203:253–310.

Kuwada, J.Y., R.R. Bernhardt, and N. Nguyen. 1990. Development of spinal neurons and tracts in the zebrafish embryo. *J. Comp. Neurol.* 302:617–628.

Lamborghini, J.E. 1980. Rohon-beard cells and other large neurons in *Xenopus* originate during gastrulation. *J. Comp. Neurol.* 189:323–333.

Le, T.T., D.D. Coovert, U.R. Monani, G.E. Morris, and A.H.M. Burghes. 2000. The survival motor neuron (SMN) protein: effect of exon loss and mutation on protein localization. *Neurogenetics.* 3:7–16.

Lefebvre, S., L. Burglen, S. Reboullet, O. Clermont, P. Burlet, L. Viollet, B. Benichou, C. Cruaud, P. Millasseau, M. Zeviani, et al. 1995. Identification and characterization of a spinal muscular atrophy-determining gene. *Cell.* 80: 155–165.

Lefebvre, S., P. Burlet, Q. Liu, S. Bertrandy, O. Clermont, A. Munnich, G. Dreyfuss, and J. Melki. 1997. Correlation between severity and SMN protein level in spinal muscular atrophy. *Nat. Genet.* 16:265–269.

Liu, Q., and G. Dreyfuss. 1996. A novel nuclear structure containing the survival of motor neurons protein. *EMBO J.* 15:3555–3565.

Liu, S., W. Lu, T. Obara, S. Kuida, J. Lehoczky, K. Dewar, I.A. Drummond, and D.R. Beier. 2002. A defect in a novel Nek-family kinase causes cystic kidney disease in the mouse and in zebrafish. *Development.* 129:5839–5846.

Lorson, C.L., and E.J. Androphy. 1998. The domain encoded by exon 2 of the sur-

vival motor neuron protein mediates nucleic acid binding. *Hum. Mol. Genet.* 7:1269–1275.

Lorson, C.L., and E.J. Androphy. 2000. An exonic enhancer is required for inclusion of an essential exon in the SMA-determining gene SMN. *Hum. Mol. Genet.* 9:259–265.

Lorson, C.L., E. Hahnen, E.J. Androphy, and B. Wirth. 1999. A single nucleotide in the SMN gene regulates splicing and is responsible for spinal muscular atrophy. *Proc. Natl. Acad. Sci. USA.* 96:6307–6311.

Marusich, M.F., H.M. Furneaux, P.D. Henion, and J.A. Weston. 1994. Hu neuronal proteins are expressed in proliferating neurogenic cells. *J. Neurobiol.* 25:143–155.

McClintock, J.M., M.A. Kheirbek, and V.E. Prince. 2002. Knockdown of duplicated zebrafish hoxb1 genes reveals distinct roles in hindbrain patterning and a novel mechanism of duplicate gene retention. *Development.* 129:2339–2354.

Melancon, E., D.W. Liu, M. Westerfield, and J.S. Eisen. 1997. Pathfinding by identified zebrafish motoneurons in the absence of muscle pioneers. *J. Neurosci.* 17:7796–7804.

Melki, J. 1997. Spinal muscular atrophy. *Curr. Opin. Neurol.* 10:381–385.

Mendelson, B. 1986. Development of reticulospinal neurons of the zebrafish I: time of origin. *J. Comp. Neurol.* 251:160–171.

Meng, A., H. Tang, B.A. Ong, M.J. Farrell, and S. Lin. 1997. Promoter analysis in living zebrafish embryos identifies a cis-acting motif required for neuronal expression of GATA-2. *Proc. Natl. Acad. Sci. USA.* 94:6267–6272.

Metcalfe, W.K., B. Mendelson, and C.B. Kimmel. 1986. Segmental homologies among reticulospinal neurons in the hindbrain of the zebrafish larva. *J. Comp. Neurol.* 251:147–159.

Metcalfe, W.K., P.Z. Myers, B. Trevarrow, M.B. Bass, and C.B. Kimmel. 1990. Primary neurons that express the L2/HNK-1 carbohydrate during early development in the zebrafish. *Development.* 110:491–504.

Monani, U.R., C.L. Lorson, D.W. Parsons, T.W. Prior, E.J. Androphy, A.H. Burghes, and J.D. McPherson. 1999. A single nucleotide difference that alters splicing patterns distinguishes the SMA gene SMN1 from the copy gene SMN2. *Hum. Mol. Genet.* 8:1177–1183.

Monani, U.R., M. Sendtner, D.D. Coovert, D.W. Parsons, C. Andreassi, T.T. Le, S. Jablonka, B. Schrank, W. Rossol, T.W. Prior, et al. 2000. The human centromeric survival motor neuron gene (SMN2) rescues embryonic lethality in Smn(−/−) mice and results in a mouse with spinal muscular atrophy. *Hum. Mol. Genet.* 9:333–339.

Monani, U.R., M.T. Pastore, T.O. Gavrilina, S. Jablonka, T.T. Le, C. Andreassi, J.M. DiCocco, C. Lorson, E.J. Androphy, M. Sendtner, et al. 2003. A transgene carrying an A2G missense mutation in the SMN gene modulates phenotypic severity in mice with severe (type I) spinal muscular atrophy. *J. Cell Biol.* 160:41–52.

Myers, P.Z., J.S. Eisen, and M. Westerfield. 1986. Development and axonal outgrowth of identified motoneurons in the zebrafish. *J. Neurosci.* 6:2278–2289.

Nasevicius, A., and S.C. Ekker. 2000. Effective targeted gene 'knockdown' in zebrafish. *Nat. Genet.* 26:216–220.

Ono, F., S. Higashijima, A. Shcherbatko, J.R. Fetcho, and P. Brehm. 2001. Paralytic zebrafish lacking acetylcholine receptors fail to localize rapsyn clusters to the synapse. *J. Neurosci.* 21:5439–5448.

Pagliardini, S., A. Giavazzi, V. Setola, C. Lizier, M. Di Luca, S. DeBiasi, and G. Battaglia. 2000. Subcellular localization and axonal transport of the survival motor neuron (SMN) protein in the developing rat spinal cord. *Hum. Mol. Genet.* 9:47–56.

Parsons, M.J., I. Campos, E.M. Hirst, and D.L. Stemple. 2002. Removal of dystroglycan causes severe muscular dystrophy in zebrafish embryos. *Development.* 129:3505–3512.

Pike, S.H., E.F. Melancon, and J.S. Eisen. 1992. Pathfinding by zebrafish motoneurons in the absence of normal pioneer axons. *Development.* 114:825–831.

Roberts, D.F., J. Chavez, and S.D.M. Court. 1970. The genetic component in child mortality. *Arch. Dis. Child.* 45:33–38.

Rossoll, W., A.K. Kroning, U.M. Ohndorf, C. Steegborn, S. Jablonka, and M. Sendtner. 2002. Specific interaction of Smn, the spinal muscular atrophy determining gene product, with hnRNP-R and gry-rbp/hnRNP-Q: a role for Smn in RNA processing in motor axons? *Hum. Mol. Genet.* 11:93–105.

Schrank, B., R. Gotz, J.M. Gunnersen, J.M. Ure, K.V. Toyka, A.G. Smith, and M. Sendtner. 1997. Inactivation of the survival motor neuron gene, a candidate gene for human spinal muscular atrophy, leads to massive cell death in early mouse embryos. *Proc. Natl. Acad. Sci. USA.* 94:9920–9925.

Terns, M.P., and R.M. Terns. 2001. Macromolecular complexes: SMN–the master assembler. *Curr. Biol.* 11:R862–R864.

Tessier-Lavigne, M., and C.S. Goodman. 1996. The molecular biology of axon guidance. *Science.* 274:1123–1133.

Thisse, C., B. Thisse, T.F. Schilling, and J.H. Postlethwait. 1993. Structure of the zebrafish snail1 gene and its expression in wild-type, spadetail and no tail mutant embryos. *Development.* 119:1203–1215.

Viollet, L., S. Bertrandy, A.L. Bueno Brunialti, S. Lefebvre, P. Burlet, O. Clermont, C. Cruaud, J.L. Guenet, A. Munnich, and J. Melki. 1997. cDNA isolation, expression, and chromosomal localization of the mouse survival motor neuron gene (Smn). *Genomics.* 40:185–188.

Weinberg, E.S., M.L. Allende, C.S. Kelly, A. Abdelhamid, T. Murakami, P. Andermann, O.G. Doerre, D.J. Grunwald, and B. Riggleman. 1996. Developmental regulation of zebrafish MyoD in wild-type, no tail and spadetail embryos. *Development.* 122:271–280.

Westerfield, M. 1995. The Zebrafish Book. University of Oregon Press, Eugene, Oregon. 307 pp.

Wills, Z., L. Marr, K. Zinn, C.S. Goodman, and D. Van Vactor. 1999. Profilin and the Abl tyrosine kinase are required for motor axon outgrowth in the *Drosophila* embryo. *Neuron.* 22:291–299.

Young, P.J., T.T. Le, N.T. Man, A.H. Burghes, and G.E. Morris. 2000a. The relationship between SMN, the spinal muscular atrophy protein, and nuclear coiled bodies in differentiated tissues and cultured cells. *Exp. Cell Res.* 256: 365–374.

Young, P.J., N.T. Man, C.L. Lorson, T.T. Le, E.J. Androphy, A.H. Burghes, and G.E. Morris. 2000b. The exon 2b region of the spinal muscular atrophy protein, SMN, is involved in self-association and SIP1 binding. *Hum. Mol. Genet.* 9:2869–2877.

Zeller, J., V. Schneider, S. Malayaman, S. Higashijima, H. Okamoto, J. Gui, S. Lin, and M. Granato. 2002. Migration of zebrafish spinal motor nerves into the periphery requires multiple myotome-derived cues. *Dev. Biol.* 252:241–256.

Zhang, H.L., F. Pan, B. Hong, S.M. Shenoy, R.H. Singer, and G.J. Bassell. 2003. Active transport of the survival motor neuron (SMN) protein and the role of exon-7 in cytoplasmic localization. *J. Neurosci.* 23:6627–6637.

The Journal of Cell Biology